IEEJ Journal of Industry Applications
Vol.6 No.6 pp.395–400 DOI: 10.1541/ieejjia.6.395

Paper

Fast Calculation of AC Copper Loss for High Speed Machines by Zooming Method

Hirokatsu Katagiri[*a)] Member, Hiroyuki Sano[*] Member
Kazuki Semba[*] Member, Noriyo Mimura[*] Non-member
Takashi Yamada[*] Member

(Manuscript received Jan. 12, 2017, revised June 16, 2017)

A model reduction method for finite element analysis such as the zooming analysis is conducted to calculate the AC copper loss of high speed electric machines. In this paper, the accuracy of the zooming method is validated by comparison with thorough analysis and the calculation speed in the zooming analysis is found to increase by 7.8 times that of thorough analysis.

Moreover, the zooming method is applied to the analysis of the copper loss of a litz wire with respect to an interior permanent magnet motor rotating at high speed. The copper loss of the litz wire could be calculated within a practical computation time.

Keywords: permanent magnet motor, copper loss, litz wire, finite element method, model reduction, zooming analysis

1. Introduction

Due to the increasing capacity and rotating speed of electric machines, the cross-section area of winding is enlarged such as the rectangular type and the frequency of the current is increased [1]. The localization of the current density is caused due to the skin and proximity effects. Estimating the AC copper loss accurately is required for improving the efficiency of the electric machines.

To estimate the AC Copper loss, models with an electrical conductivity and the accurate shape of wires are calculated by using the finite element method (FEM) because the distribution of the current density in wire is not homogeneous. Therefore, the number of elements and the calculation time increases. In particular, the 3-D finite element analysis with huge number of elements is needed in the copper loss calculation of litz wire, and it is difficult to calculate the analysis within a practical computation time.

A model reduction method (hereafter called Zooming analysis) has been proposed for the reduction of the calculation time [2][3]. In (2), the zooming method is applied to the copper loss calculation of wires in the 2D finite element analysis. In (3), the zooming method is applied to the electromagnetic force calculation in 3D finite element analysis with nodal elements. However, the zooming method has not been applied to the copper loss calculation of wires in the 3D finite element analysis with edge elements.

In this paper, the zooming method is applied for the AC copper loss calculation of an interior permanent magnet (IPM) motor and compared with the thorough analysis. This paper shows that the zooming method reduces the calculation time while the accuracy is maintained. Moreover, the zooming method is applied to the analysis of the copper loss of litz wire on the copper loss of an IPM motor rotating high speed. The copper loss of litz wire can be calculated within a practical computation time.

a) Correspondence to: Hirokatsu Katagiri. E-mail: katagiri.hirokatsu@jsol.co.jp
* Electromagnetic Engineering Department, Engineering Technology Division, JSOL Corporation
Harumi Center Bldg., 2-5-24, Harumi, Chuo-ku, Tokyo 104-0053, Japan

2. Analysis Method

2.1 Magnetic Field Analysis using FEM The equations of the magnetic field using the 3-D FEM, which are given by the magnetic field vector potential $\boldsymbol{A}$ and the electric scaler potential ϕ [4]:

$$\mathrm{rot}(\nu\,\mathrm{rot}\,\boldsymbol{A}) = \boldsymbol{J}_0 + \boldsymbol{J}_e + \nu_0\,\mathrm{rot}\,\boldsymbol{M} \quad \cdots\cdots (1)$$

$$\boldsymbol{J}_e = -\sigma\left(\frac{\partial \boldsymbol{A}}{\partial t} + \mathrm{grad}\,\phi\right) \quad \cdots\cdots (2)$$

$$\mathrm{div}\,\boldsymbol{J}_e = 0 \quad \cdots\cdots (3)$$

where $\boldsymbol{J}_0$ is the exiting current density, $\boldsymbol{J}_e$ is the eddy current, σ is the conductivity, ν is the reluctivity, ν_0 is the reluctivity of the vacuum, and $\boldsymbol{M}$ is the magnetization of the permanent magnet. In the FEM analysis, (1) and (3) are discretized by using the Galerkin Method [5] and the matrix is solved by ICCG method [4], which is linear iterative solver. If there are materials with nonlinear magnetic properties such as irons in the analysis region, it is necessary to iterate the calculation of those equations by Newton-Raphson method.

In the case of the magnetic field coupled with the electrical circuit [6], (1), (3) and the following equation, which are given by circuit current I, are solved simultaneously:

$$V - RI - \nu_{coil} = 0 \quad \cdots\cdots (4)$$

where V is the voltage source, R is the resistance, ν_{coil} is the

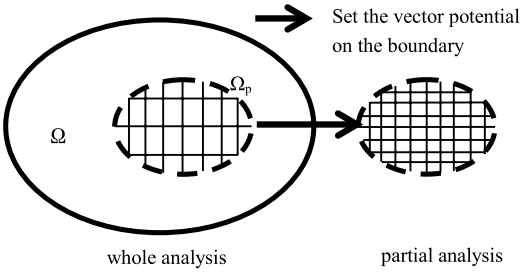

Fig. 1. Zooming analysis

induced voltage of the coil in the FEM region [7].

2.2 Zooming Analysis Figure 1 shows the conceptual diagram of zooming analysis. The zooming analysis performs finite element analysis twice. In the first analysis (hereafter called whole analysis), in order to calculate whole field, whole region is modeled. Using zooming method allows to use rough mesh and to simplify the detailed shape. In the second analysis (hereafter called partial analysis), a part of the whole region whose field is calculated accurately is modeled. In order to calculate results accurately, the fine element mesh is used and the detailed shape is modeled. In the partial analysis, the vector potential obtained from the analysis of the whole model is used as the Dirichlet boundary condition. It means partial model boundary is given flux density of whole model. The characteristics of the method are shown in this appendix.

2.3 Application for Copper Loss Calculation of Motors The zooming method is used in order to calculate AC copper loss for high speed machines. The whole model and the partial model are made as follows.

In the whole analysis, the eddy current in coils is not taken into account. Therefore, the coils can be modeled as a bulk. The whole model can be calculated by short calculation time because the whole analysis can use the rough mesh in coil region and to simplify the shape of wire. The exiting current flows in the coil.

In the partial analysis, only wires and surrounding air are modeled. It models the shape of each wire and the eddy current in wires is calculated. In order to express the current flowing between wires, the circuit is coupled with the FEM, which is solved by (1), (3) and (4) simultaneously. In the partial analysis, there are no materials with nonlinear magnetic properties such as irons. Therefore, the calculating time becomes short because the nonlinear iterations are not needed.

3. AC Copper Loss Calculation of an IPM Motor

In this chapter, in order to show that the method reduces the calculation time while the accuracy is maintained, the zooming analysis is conducted to calculate the AC copper loss of the IPM motor [8] shown in Fig. 2(a), and the analysis condition is shown in Table 1. The result and the calculation time are compared with the thorough model.

3.1 Analysis Model and Conditions The 2-Dimentional transient finite element analysis is conducted with the current input. Figure 2(a) shows thorough analysis model. The thorough analysis means normal FEM analysis. The diameter of the wires is 1.3 mm. The number of coil turns is 35 per one slot and the wires connected in serial. By changing

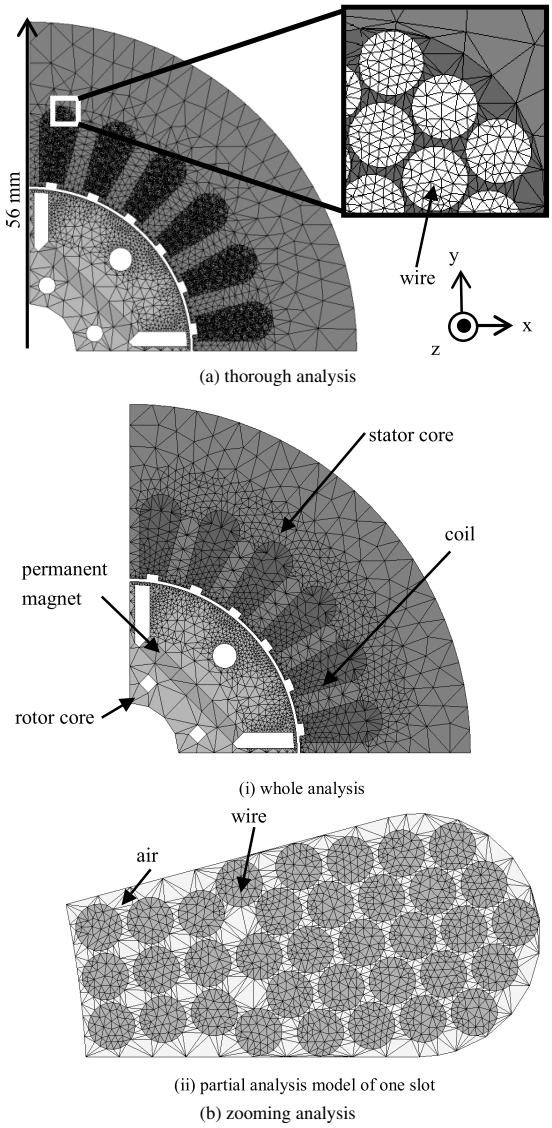

(a) thorough analysis

(i) whole analysis

(ii) partial analysis model of one slot

(b) zooming analysis

Fig. 2. Analysis models

Table 1. Analysis condition

Number of poles	4
Coil current (A_{rms})	3
Coil turn per slot (turn)	35
Number of slots	24
residual magnetic flux density of magnet (T)	1.25
rotation speed (r/min)	500, 1,000, 3,000, 5,000, 10,000

the rotation speed from 500 to 10,000 r/min, six cases are calculated. Figure 2(b)(i) shows the model of the whole analysis and the one of the partial model of one slot is shown in Fig. 2(b)(ii). In the partial model, 6 slots are calculated. The time interval is 1/192 of one cycle period. In the whole analysis, the coils are modeled as a bulk and each wire is modeled in the partial analysis. The whole analysis does not take into account the eddy current. Therefore, the six different speeds of the partial analysis can be used the same result of the whole analysis.

3.2 Results Figure 3 shows the distribution of copper loss in the wires calculated by zooming analysis. The loss in

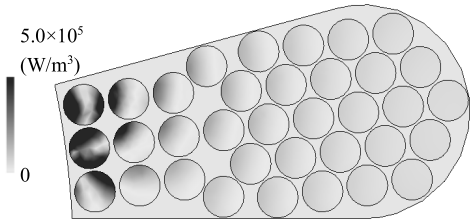

Fig. 3. Distribution of copper loss (10,000 r/min)

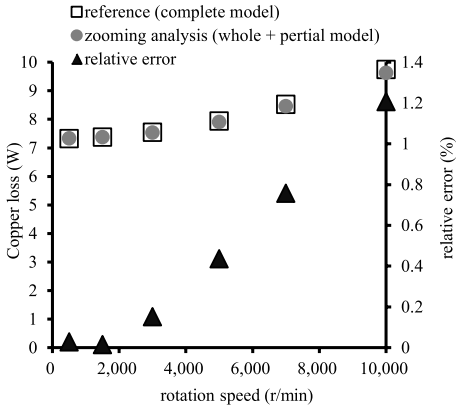

Fig. 4. Copper loss characteristics

Table 2. Calculation time

Analysis	Thorough	Zooming analysis	
		Whole	Partial
Number of elements	24,679	5,329	18,702
Number of average ICCG iterations pre one time step	304	180	52
Number of time steps per one case	220	192	220
Number of calculation cases	6	1	6
Calculation time (min.)	334.4	42.8	

wires can be calculated. The non-homogeneous copper loss distribution in the wires caused by proximity effect and skin effect can be calculated.

Figure 4 shows the copper loss characteristics. The relative error means the differences between the copper losses calculated by the zooming analysis and that calculated by the thorough model. The copper loss increases as the rotation speed increases. The error of the zooming analysis compared with the thorough model is no more than 1.2% if the rotation speed increases under 10,000 r/min.

The calculation time is shown in Table 2. Those results are obtained by the multithreaded parallel processing with 4 cores [9]. The zooming analysis calculated six different speeds in approximately 1/8 of the time of the thorough model because of the following advantages in zooming analysis.

1. The partial analyses of six different speeds can use the same result of the whole analysis.
2. The number of unknowns decreases because the coil of the whole model is modeled as a bulk and only the slot is modeled in the partial model.
3. The number of ICCG iterations decreases because the number of unknowns decreases in whole model, the partial analysis does not need nonlinear iterations.

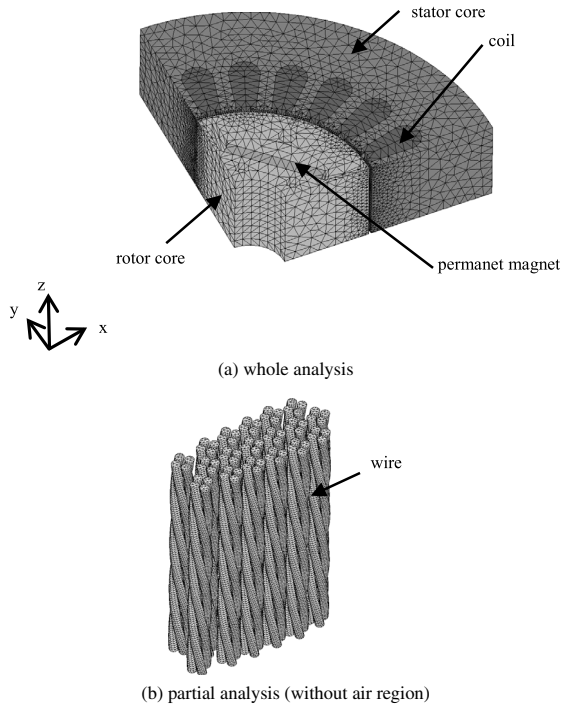

Fig. 5. Analysis models of the litz wire model

4. The number of time steps is only one cycle period in whole region analysis because there is no transient state. In contrast, the number of time steps of the thorough analysis and the partial analysis approximately 1.1 cycle periods in order to obtain steady states.

4. AC copper Loss Calculation of LITZ WIRE

In case of the copper loss calculation of the litz wire, the 3D FEM is needed to calculate eddy currents in twisted wires. In this case, the meshes of the 3D FEM become too large, and the calculation time in thorough analysis becomes too long by thorough analysis.

In this chapter, the zooming method is applied to the copper loss calculation of litz wire on the IPM motor rotating high speed in order to reduce the calculation time.

4.1 Analysis Model and Conditions Figure 5 shows the analysis models of litz wire model. The model is the same as that of chapter III without wires.

In the whole analysis as shown in Fig. 5(a), the coils are modeled as a bulk. The model is 1/3 of whole region, which corresponds to one twist pitch, by the symmetry of axial direction. The magnetic field of the coil slot is synchronous field. Therefore, the copper losses of those slots are almost the same. In the partial analysis, the wires of 1 slot are modeled as shown in Fig. 5(b). The number of turns per one slot is 18. The coil consists of 4 wires. The wires connected in parallel. The wire arrangement in one slot is shown in Fig. 6. The wire of the same number means same wire. The diameter of the wires is 0.7 mm. The twist pitch is 20 mm. The rotation speeds are from 500 to 10,000 r/min.

In order to clarify the effects of litz wire, the IPM motor with no twisted wires (hereafter called parallel wire model) is analyzed. The other conditions and the other model shape of the parallel wire model are same as those of the litz wire model. In the parallel wire model, the 2-D finite element

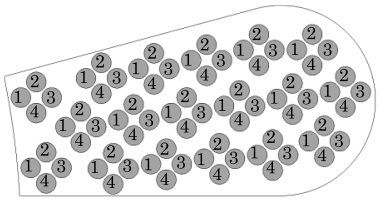

Fig. 6. The wire arrangement of one slot

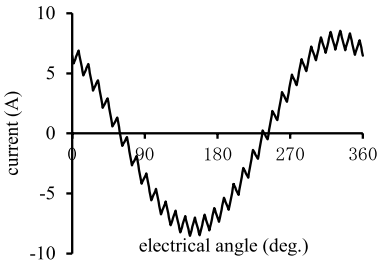

Fig. 7. Input current waveform in W phase (10,000 r/min)

Table 3. Calculation time and number of elements in litz wire model

analysis	thorough	zooming	
		whole	partial
Number of elements	3,878,995	182,147	639,319
Calculation time (hours)	1871.1	5.59	8.42
		14.0	

Used CPU:Xeon E5-1660 v3×8 cores

analysis is used because the symmetry of the axial direction.

The coil current is the three-phase AC. The current waveform in W phase is shown in Fig. 7. The coil current is sinusoidal waveform with high harmonics caused by the inverter. The frequency of the fundamental harmonic and the carrier harmonics are 333 Hz and 10 kHz at 10,000 r/min, respectively.

4.2 Results Figure 8 shows the current of each wire. The figure's number means the current of the same number's wire in Fig. 6. In parallel wire model, the currents of the wire differ from each other. The reasons are follows. The electromotive force causes the magnetic flux between the wires. The current flows between the wires due to electromotive force, which is called as circulating current. In parallel wire model, the currents of the wire differ from each other due to circulating current [10]. In contrast, in the litz wire model, the magnetic flux between the wires is canceled by the twist. Therefore the currents of the wire are almost the same. The total currents of parallel wire and litz wire are the same.

The copper losses are shown in Fig. 9. Under 5,000 r/min, the copper loss of litz wire model is larger than that of parallel wire model because of the DC resistance. In 10,000 r/min, the copper loss of the litz wire model decrease by 9% compared with that of the parallel wire model because of canceling out circulating current.

Table 3 shows the number of elements and the calculation time in the litz wire model. Those results are obtained by the multithreaded parallel processing with 8 cores. The number of elements of whole model is less than that of the

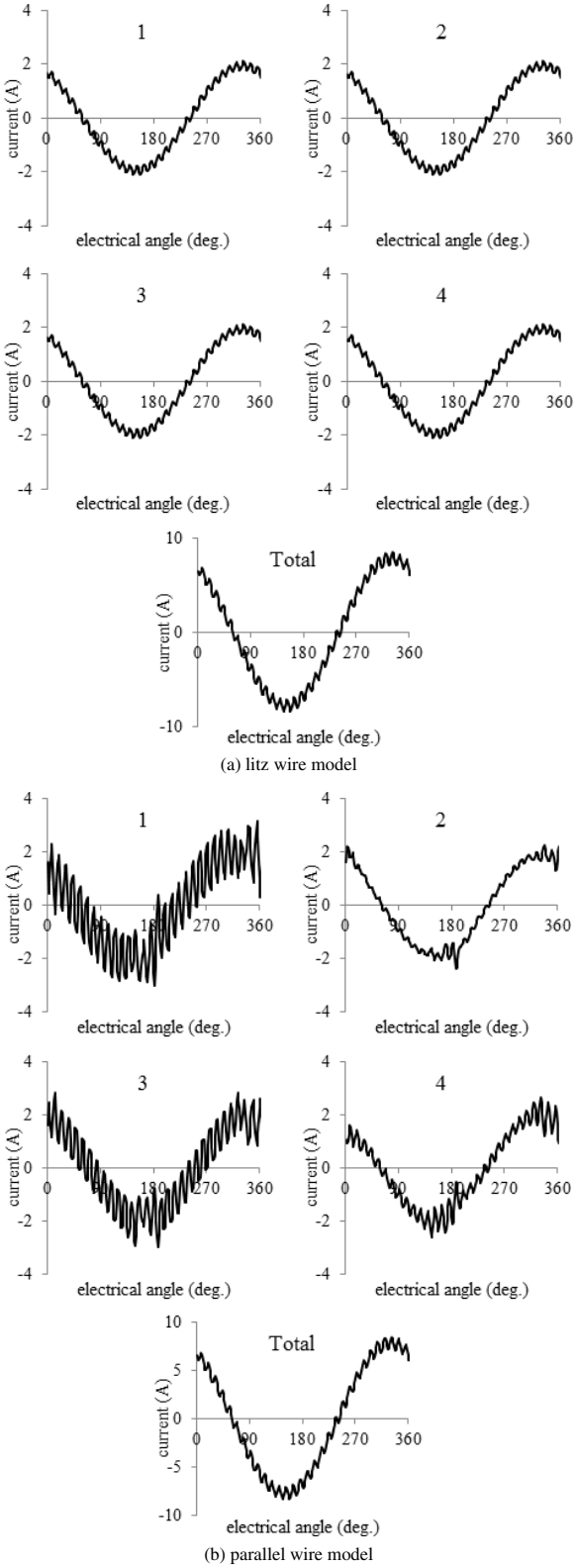

(a) litz wire model

(b) parallel wire model

Fig. 8. Current waveform in strands of W phase (10,000 r/min)

thorough model whole model because the coils are modeled as a bulk. The number of elements of partial model is less than that of the thorough model because of using the symmetry. The calculation time of the zooming analysis is 1/133 of that of the thorough analysis. The calculation time of the zooming analysis is 14.0 hours. The eddy current loss of the

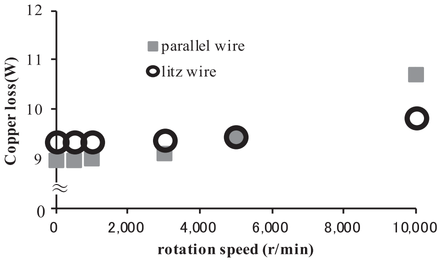

Fig. 9. Copper L oss (W)

litz wire model can be calculated by the zooming analysis at 8.42 hours.

5. Conclusion

The zooming method is applied to the AC copper loss calculation of an IPM motor and the results is compared with the thorough analysis. It shows that the method reduces the calculation time while the accuracy is maintained. Moreover, we show the copper loss of the litz wire model can be calculated by the zooming analysis within a practical computation time.

The error of the zooming analysis compared with the thorough model was less than 1.2%. The zooming analysis can be reduced the number of elements, nonlinear iteration, the number of time steps of whole region, the number of calculation cases of whole region. Therefore, the zooming analysis calculated six different speeds in approximately 1/8 of the time of the thorough model. The calculation time of litz wire model of the zooming analysis was 14.0 hours by using 8 cores of Xeon E5-1660 v3 CPU.

References

(1) N. Bianchi, S. Bolognani, and F. Luise: "Potentials and limits of high-speed PM motors", *IEEE Trans. on Industry*, Vol.52, No.3 (2015)

(2) M. Al Eit, F. Bouillault, C. Marchand, and G. Krebs: "2D Reduced Model for eddy currents calculation in Litz Wire and Its Application for Switched Reluctance Machine", *IEEE Trans. Magn.*, Vol.52, No.3 (2015)

(3) T. Narita, M. Kawabe, and Y. Shimomura: "Magnetostatic Analysis by the Zooming method", The Papers of Joint Technical Meeting on Static Apparatus and Rotating Machinery, IEE Japan, SA-92-15, RM-92-50, pp.119–128 (1992) (in Japanese)

(4) K. Fujiwara, T. Nakata, and H. Ohashi: "Improvement of Convergence Characteristics of ICCG Method for A-f Method using Edge Element", *IEEE Trans. Magn.*, Vol.32, No.3, pp.804–807 (1996)

(5) O.C. Zienkiewicz and R.L. Taylor: "THE FINITE ELEMENT METHOD", Butterworth-Heinemann (1967)

(6) T. Nakata, N. Takahashi, K. Fujiwara, and A. Ahagon: "-D finite element method for analyzing magnetic fields in electrical machines excited from voltage sources", *IEEE Trans. Magn.*, Vol.24, No.6, pp.2582–2584 (1988)

(7) N.M. Abe, J.R. Cardoso, and A. Foggia: "Coupling Electric Circuit and 2D-FEM Model With Dommel's Approach for Transient Analysis", *IEEE Trans. Magn.*, Vol.34, No.5, pp.1448–1451 (1998)

(8) Y. Kawase T. Yamaguchi, S. Sano, M. Igata, K. Ida, and A. Yamagiwa: "3-D eddy current analysis in a silicon steel sheet of an interior permanent magnet motor", *IEEE Trans. Magn.*, Vol.39, No.3, pp.1448–1451 (2003)

(9) K. Semba, K. Tani, T. Yamada, T. Iwashita, Y. Takahashi, and H. Nakashima: "Parallel Performance of Multi-threaded ICCG Solver in Electromagnetic Finite Element Analyses on the Latest Processors", In Proc. Progress In Electromagnetics Research Symposium, pp.979–983 (2013)

(10) Y. Kawase T. Yamaguchi, D. Kato, S. Tsukada, K. Ida, K. Ito, Y. Fukui, and N. Nishikawa: "3-D Finite Element Analysis of Eddy Current Loss in Stranded Wire Coil Using Earth Simulator", Sensors & Transducers, Vol.197, No.2, pp.20–27 (2016)

(11) B. Spain: "Vector Analysis", Van Nostrand Reinhold Inc., U.S. (1968)

Appendix

In this appendix, the characteristics of zooming method, which uses the Dirichlet boundary condition, is described by the numerical approach.

In this method, the results of the partial analysis is the same as those of the thorough analysis if the materials properties and source current of the partial analysis are the same as those of the thorough analysis.

In order to clarify the above, we submit that the solution is uniquely determined if the vector potential on the boundary of the partial analysis is determined.

The analysis region is made by the same material with linear magnetic permeability μ and linear electrical permeability σ.

The equation of the Maxwell-Ampere's law and the Faraday's law of induction can be written as follows, which are given by the magnetic field $\boldsymbol{H}$ and the electric field $\boldsymbol{E}$.

$$\mathrm{rot}\,\boldsymbol{H} - \sigma\frac{\partial \boldsymbol{E}}{\partial t} = \boldsymbol{J}_0 \quad \text{(A1)}$$

$$\mathrm{rot}\,\boldsymbol{E} + \frac{\partial(\mu\boldsymbol{H})}{\partial t} = \boldsymbol{0} \quad \text{(A2)}$$

It is assume that two solutions of $\boldsymbol{E}$ and $\boldsymbol{H}$ satisfied with (A1) and (A2) exist in the condition of using the same initial value. Let two solutions of $\boldsymbol{E}$ be $\boldsymbol{E}_1$ and $\boldsymbol{E}_2$, and let the difference of those be $\boldsymbol{E}_d$. Let two solutions of $\boldsymbol{H}$ be $\boldsymbol{H}_1$ and $\boldsymbol{H}_2$, and let the difference of those be $\boldsymbol{H}_d$.

$$\boldsymbol{E}_d = \boldsymbol{E}_1 - \boldsymbol{E}_2 \quad \text{(A3)}$$

$$\boldsymbol{H}_d = \boldsymbol{H}_1 - \boldsymbol{H}_2 \quad \text{(A4)}$$

The following equation is satisfied because the set of $\boldsymbol{E}_1$ and $\boldsymbol{H}_2$ and the set of $\boldsymbol{E}_2$ and $\boldsymbol{H}_2$ are satisfied with (A1) and (A2), respectively.

$$\mathrm{rot}\,\boldsymbol{H}_d - \sigma\frac{\partial \boldsymbol{E}_d}{\partial t} = \boldsymbol{0} \quad \text{(A5)}$$

$$\mathrm{rot}\,\boldsymbol{E}_d + \frac{\partial(\mu\boldsymbol{H}_d)}{\partial t} = \boldsymbol{0} \quad \text{(A6)}$$

The following equations can be obtained by taking an inner product with $\boldsymbol{E}_d$ and $\boldsymbol{H}_d$ on the both sides of (A5) and (A6), respectively.

$$\boldsymbol{E}_d \cdot \mathrm{rot}\,\boldsymbol{H}_d - \boldsymbol{E}_d \cdot \sigma\frac{\partial \boldsymbol{E}_d}{\partial t} = \boldsymbol{0} \quad \text{(A7)}$$

$$\boldsymbol{H}_d \cdot \mathrm{rot}\,\boldsymbol{E}_d + \boldsymbol{H}_d \cdot \frac{\partial(\mu\boldsymbol{H}_d)}{\partial t} = \boldsymbol{0} \quad \text{(A8)}$$

The following equation can be obtained by subtracting (A7) from (A8).

$$\boldsymbol{H}_d \cdot \mathrm{rot}\,\boldsymbol{E}_d + \boldsymbol{H}_d \cdot \frac{\partial(\mu\boldsymbol{H}_d)}{\partial t} = \boldsymbol{E}_d \cdot \mathrm{rot}\,\boldsymbol{H}_d - \boldsymbol{E}_d \cdot \sigma\frac{\partial \boldsymbol{E}_d}{\partial t} \quad \text{(A9)}$$

The vector formula is shown as follows [11].

$$\mathrm{div}(\boldsymbol{F}\times\boldsymbol{G}) = \boldsymbol{G}\cdot\mathrm{rot}\,\boldsymbol{F} - \boldsymbol{F}\cdot\mathrm{rot}\,\boldsymbol{G} \quad \text{(A10)}$$

where $\boldsymbol{F}$, $\boldsymbol{G}$ means vectors.

The following equation can be obtained by (A9) and (A10).

$$\frac{1}{2}\frac{\partial}{\partial t}(\mu \boldsymbol{H}_d \cdot \boldsymbol{H}_d + \sigma \boldsymbol{E}_d \cdot \boldsymbol{E}_d) = \mathrm{div}(\boldsymbol{H}_d \times \boldsymbol{E}_d) \cdots\cdots \text{(A11)}$$

The following equation can be obtained by integrating (A11) on the analysis region D.

$$\frac{1}{2}\frac{\partial}{\partial t}\int_D (\mu \boldsymbol{H}_d \cdot \boldsymbol{H}_d + \sigma \boldsymbol{E}_d \cdot \boldsymbol{E}_d) dV = \int_D \mathrm{div}(\boldsymbol{H}_d \times \boldsymbol{E}_d) dV \cdots\cdots\cdots\cdots\cdots\cdots \text{(A12)}$$

The following equation is the necessary and sufficient condition that $\boldsymbol{E}_d$ and $\boldsymbol{H}_d$ be zero in all regions of D.

$$\int_D (\mu \boldsymbol{H}_d \cdot \boldsymbol{H}_d + \sigma \boldsymbol{E}_d \cdot \boldsymbol{E}_d) dV = 0 \cdots\cdots\cdots\cdots \text{(A13)}$$

The following equation can be obtained by taking the time derivative of (A13).

$$\frac{\partial}{\partial t}\int_D (\mu \boldsymbol{H}_d \cdot \boldsymbol{H}_d + \sigma \boldsymbol{E}_d \cdot \boldsymbol{E}_d) dV = 0 \cdots\cdots\cdots \text{(A14)}$$

(A13) is satisfied at initial time because of using the same initial value. Therefore, if (A14) is satisfied in all time, then (A13) is satisfied in all time.

In order to satisfy (A14) in all time, it is necessary to be zero in the right side of (A11) zero. Thus, the condition to determine $\boldsymbol{E}$ and $\boldsymbol{H}$ uniquely is obtained in the following equation.

$$\int_D \mathrm{div}(\boldsymbol{H}_d \times \boldsymbol{E}_d) dV = 0 \cdots\cdots\cdots\cdots\cdots\cdots \text{(A15)}$$

Using divergence theorem in (A15), the following equation can be obtained.

$$\int_{\partial D} (\boldsymbol{H}_d \times \boldsymbol{E}_d) \cdot \boldsymbol{n} dS = 0 \cdots\cdots\cdots\cdots\cdots\cdots \text{(A16)}$$

where ∂D is the boundary of D, $\boldsymbol{n}$ is the outward normal vector.

The following equation can be obtained by deforming (A16).

$$\int_{\partial D} (\boldsymbol{E}_d \times \boldsymbol{n}) \cdot \boldsymbol{H}_d dS = 0 \cdots\cdots\cdots\cdots\cdots\cdots \text{(A17)}$$

Hence, if $\boldsymbol{E}$ on the boundary is determined uniquely, $\boldsymbol{E}$ and $\boldsymbol{H}$ are determined uniquely.

$\boldsymbol{E}$ is expressed by $\boldsymbol{A}$ and ϕ in A-ϕ method as following equation.

$$\boldsymbol{E} = -\left(\frac{\partial \boldsymbol{A}}{\partial t} + \mathrm{grad}\,\phi\right) \cdots\cdots\cdots\cdots\cdots\cdots\cdots\cdots \text{(A18)}$$

Therefore, if the tangential component of $\boldsymbol{A}$ and ϕ is determined on the boundary, $\boldsymbol{E}$ and $\boldsymbol{H}$ are determined uniquely. If the materials on the boundary of the partial analysis are air, it is necessary to determine only the tangential component of $\boldsymbol{A}$ because ϕ is zero on the boundary.

From the above, in this zooming method, the results of the partial analysis are the same as those of the thorough analysis if the materials properties and source current of the partial analysis are the same as those of the thorough analysis.

Hirokatsu Katagiri (Member) was born in Gifu, Japan, on March 3, 1987. He received a Dr. Eng. Degree from Gifu University in 2014. He joined JSOL Corporation in 2004. He has been engaged in development of magnetic field analysis using the finite element method. He is a member of the Institute of Electrical Engineers of Japan and IEEE.

Hiroyuki Sano (Member) was born in Japan, 1975. He received the M.Sc. degree in graduate school of science from the University of Tokyo in 2000. He joined JSOL Corporation in 2000 and has been working for the development of the electromagnetic simulation software JMAG. He worked as a visiting scholar in Wisconsin Electric Machines and Power electronics Consortium (WEMPEC) during 2008–2009.

Kazuki Semba (Member) was born in 1975. He received a MC degree from Waseda University in 2001. He joined The Japan Research Institute, Limited (currently names JSOL Corporation) in 2001. He has been engaged in development of magnetic field analysis in engineering business division. He received a Dr. Informatics from Kyoto University in 2015. He is a member of the Institute of Electrical Engineers of Japan and IEEE and Gas Turbine Society of Japan.

Noriyo Mimura (Non-member) was born on October, 10, 1976. He received a MC degree from Gifu University in 2001. He joined The Japan Research Institute, Limited (currently names JSOL Corporation) in 2001. He has been engaged in development of magnetic field analysis in engineering business division.

Takashi Yamada (Member) received a MC degree from Tokyo Metropolitan University in 1987. He joined The JAIS, Limited (currently names JSOL Corporation) in 1987. He has been engaged in development of magnetic field analysis in engineering business division. He received a Dr. Eng. He is a member of the Institute of Electrical Engineers of Japan and IEEE.